UNITECH SELECTED PAPERS

International Scientific Conference
UNITECH`2024

STRUCTURAL AND DYNAMIC PROPERTIES OF ALUMINUM NANOPARTICLES DURING THE MELTING PROCESS

Unal Domekeli[1*], Murat Celtek[2]

[1]*Dept. of Physics, Trakya University, 22030, Edirne – TÜRKİYE*
[2]*Faculty of Education, Trakya University, 22030, Edirne – TÜRKİYE*

** Corresponding author: unaldomekeli@trakya.edu.tr*

Abstract

In recent years, nanoparticles, which play an important role in the development of nanotechnology, have been the focus of attention of many researchers. Metallic nanoparticles have many unique physical and chemical properties such as high thermal and electrical conductivity, high flexibility and strength, optical transmittance and chemical inertness compared to bulk materials due to surface effects. For the development and production of new nano-technological devices, a good understanding of the thermal, mechanical and electronic properties of nanoparticles is required. In this study, we investigated the structural and dynamic properties of metallic aluminum (Al) nanoparticles during the melting process using classical molecular dynamics (MD) simulation technique. In MD simulations, the interactions between Al atoms were described using embedded atom potentials (EAM). In order to observe how the thermal, structural and dynamic properties of Al nanoparticles change depending on the particle size and temperature, the potential energy, pairs distribution function, mean square displacement and diffusion coefficient of the system were calculated. The results obtained from MD simulations clearly showed that the melting point of nanoparticle increases as the particle size increases, and the structural and dynamic properties are directly related to the particle size and temperature.

Keywords: Aluminum nanoparticles, MD simulations, melting process, EAM potentials.

INTRODUCTION

Reacting metallic nanoparticles (NP) have recently become the focus of attention of many researchers as they play an important role in the development of some production technologies in the industry [1–4]. Since the development of these products is directly related to the thermodynamic history of the reacting metallic NPs, a model needs to be developed to explain thermal events such as melting and evaporation of these NPs [1]. At the nanoscale, particles exhibit many thermo-physical properties that are different from those found at the microscale. As the size decreases beyond a critical value due to the increase in the surface area-to-volume ratio, the melting temperature deviates from the bulk value and becomes a size-dependent property. The decrease in the size of metallic NPs causes a significant decrease in the melting temperature. This can deeply affect the chemical activities of the nanoparticle [2].

Al NPs are a frequently used material in reacting metallic nanoparticle applications due to their exceptional energetic properties such as increased catalytic activity and higher reactivity [3,5]. The melting temperature of these particles plays an important role in determining the ignition and combustion temperature of metal-based energetic materials. Therefore, it is important to characterize the particle size-dependent melting process of Al NPs. Due to the difficulty of performing thermal experiments on nanomaterials, many researchers have recently used MD simulation techniques to study the thermal properties of Al NPs [3,4,6,7]. Liu et al. [3] investigated the relationship between defect concentration and extra storage energy in Al NPs using MD simulation method with reactive force field. They found that as the

doi: www.doi.org/10.70456/FPWL9501

defect concentration increases, the extra storage energy increases and after melting, the extra storage energy almost disappears. Puri et al. [6], the effects of surface charge development on the melting of Al NPs were investigated by MD simulation using different interaction potentials. They reported that the melting points of Al particles have a linear relationship with the particle size and the evolution of surface charges during the melting process is negligible. In this study, structural and dynamic properties of metallic Al NPs such as potential energy, pair distribution function (PDF), square mean displacement (MSD) and diffusion coefficient were investigated during the melting process using MD simulation with EAM force field.

EXPOSITION

In MD simulations, EAM potentials are frequently used, which can accurately describe the interatomic interactions for metals and their alloys. According to the EAM model, the total energy of a system consisting of N atoms is written as [8]:

$$E_T = \sum_{i=1}^{N}\left[\frac{1}{2}\sum_{i\neq j}^{N}\phi(r_{ij}) + F_i(\rho_i)\right] \quad (1)$$

where $\phi(r_{ij})$ is the pair interaction potential energy function and $F_i(\rho_i)$ is the energy required to place an atom i at a lattice point where the electronic charge density ρ_i is located. This energy is called the embedding energy. ρ_i is the sum of the atomic charge densities of the neighboring atoms surrounding atom i. r_{ij} is the distance between atoms i and j. In the literature, there are both analytical and numerical EAM potential energy functions that have been successfully used in MD simulations. In this study, we used the EAM potential data developed by Sheng [9] to describe the interactions between Al atoms. All MD simulations for Al NPs and bulk system were performed using DLPOLY parallel code simulation package [10]. In order to observe the effect of particle size on the thermal, structural and dynamic properties of Al NPs during the melting process, three different sized NPs were studied. The diameters (or numbers of atom) of the nanoparticles labeled NP-1, NP-2 and NP-3 used as models in MD simulations were 3.0 nm (856 atoms), 5.1 nm (4028 atoms) and 10.0 nm (31544 atoms), respectively. Al NPs were extracted from an ideal face-centered cubic (fcc) crystal structure of size $25a_o\,x25a_o\,x25a_o$ using a series of spherical cutoff radii (a_o=4.05Å for Al [11]). The NPs were simulated under constant volume and constant temperature NVT ensemble without periodic boundary conditions, while the bulk system was simulated under constant temperature and constant pressure NPT ensemble with periodic boundary conditions. The classical equations of motion are integrated using the Leapfrog-Verlet algorithm with a time step of 1fs. The temperature and pressure of the system are controlled by the Nose-Hoover thermostat [12] and the Berendsen borastat [13], respectively. The stable structure at 0 K was obtained by first annealing the initial configuration at T=300 K using 100000 MD time steps and then cooling it to T=0 K with a cooling rate of 0.05 K/ps. The annealed nanoparticle is almost identical to the initial configuration except for the relaxed surface atoms. For each NP and bulk, the system was subjected to a heating process consisting of a series of MD simulations with a temperature increase of ΔT=100 K. Around the melting point, the temperature increment was reduced to ΔT=10 K, taking into account large temperature fluctuations. Simulations were performed at each temperature for 100000 MD time steps. The first 50000 MD time step of the 100000 MD time step was used to equilibrate the system and the last 50000 MD time step was used to generate the time averaged features.

In the Results section, we first discuss the thermal properties which are frequently used to determine the first-order phase transition. As it is known, the melting point of a system can be easily estimated

Table 1. *Physical quantities obtained from MD simulation for Al NPs and bulk system.*

Nanoparticles	N	T_m (K)	ΔH_m(Kj/mol)	a_o(Å)	E_{coh}(eV)
NP-1	856	690	6.61		
NP-2	4028	730	7.20		
NP-3	31544	760	7.52		
Bulk system					
MD	1372	930	8.81	4.048	3.360
Experimental		933.5 [11]	10.70 [14]	4.050 [11]	3.390 [11]

from the characteristic behavior of the caloric curves with temperature. For this purpose, the temperature-dependent change curves of potential energy for Al nanoparticles and bulk system are shown in Figure 1.

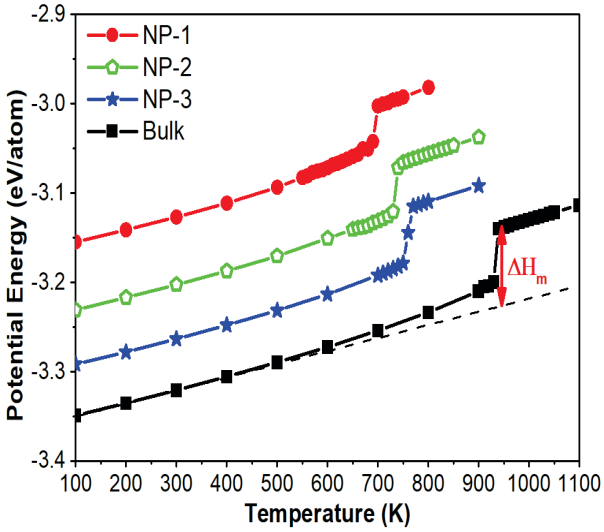

Fig. 1. *Temperature dependence of potential energy for Al NPs and bulk system.*

The potential energy for NPs and bulk system increases linearly with increasing temperature. This linear behavior breaks down with increasing temperature and a sudden increase in potential energy occurs. The temperature at which this sudden increase occurs is defined as the melting temperature at which the first-order phase transition occurs. As temperatures higher than the melting point increase, the linear behavior between potential energy and temperature continues. The potential energies of NPs are higher than that of bulk due to their high surface energy. Also, as the particle size decreases, the potential energy increases. Some physical quantities such as melting temperature (T_m), heat of fusion (ΔH_m), lattice constant (a_o) and cohesive energy (E_{coh}) obtained from MD simulation for Al NPs and bulk system are listed in Table 1 comparison with available experimental data [11,14]. The T_m predicted from the characteristic behavior of caloric curves for Al NPs are lower than those for bulk Al. Also, T_m decreases as the size of the NP decreases. The T_m obtained from MD simulation for bulk Al is in good agreement with the experimental value. As shown in Figure 1, the ΔH_m was obtained by calculating the energy difference between the solid phase and the liquid phase. The ΔH_m of bulk Al obtained from MD simulation is larger than that of NPs and is consistent with the experimental result. ΔH_m increases as the size of NP increases. The most basic parameters representing a crystal structure are a_o and E_{coh}. As can be seen from Table 1, a_o and E_{coh} obtained from MD simulations for bulk Al are in good agreement with the experimental results. This result shows that the EAM potential used to describe the interactions between Al atoms in the MD simulation can accurately describe the structure of the system at low temperatures (around room temperature). In other words, we can say that the MD simulations performed using the EAM potential produce accurate results for Al NPs and the bulk system. The PDF describes the probability of finding another particle at a distance r from a reference atom (or particle). PDF depends greatly on the type of matter, thus it varies greatly for solids, amorphous, liquids and gases. Therefore, PDF is the most important structural function that is frequently used to analyze structural properties, whether the system in question is crystalline or non-

crystalline. The expression of the PDF, $g(r)$, is as follows [15]:

$$g(r) = \frac{\Omega}{N^2}\left\langle \sum_{i}^{N}\sum_{i\neq j}^{N} \delta(r - r_{ij}) \right\rangle \quad (2)$$

where N and Ω represent the number of atoms, and volume of the simulations cell, respectively. In order to test whether the EAM potential that we used to describe the interatomic interactions in MD simulations correctly describes the system at high temperatures, the PDF of liquid bulk Al obtained from the MD simulation in Figure 2 was compared with the experimental result [16].

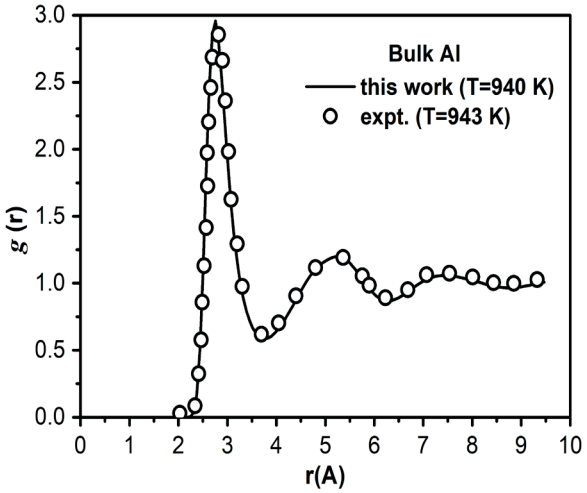

Fig. 2. *The PDFs of liquid bulk Al simulated under 0 GPa pressure.*

As can be seen from Figure 2, both MD and experimental PDFs show the characteristic behavior of the liquid phase. The MD results are in excellent agreement with the experimental result. This result is a clear evidence that the EAM potential data used in MD simulations are quite successful in describing the physical properties of bulk Al in the solid phase at low temperatures and in the liquid phase at high temperatures. Figure 3 shows the PDFs of Al NP-3 at different temperatures. At 300 K, the PDF shows the characteristic behavior of an ideal fcc crystal structure. While the peak amplitudes of the PDF decrease with increasing temperature, the peak widths increase. At 760 K, PDF cannot fully characterize either the crystalline phase or the liquid phase. As is known, a system exhibits both the solid phase and the liquid phase at the melting point. From the PDFs behavior for Al NP-3, the temperature at which these two phases coexist is 760 K. This temperature corresponds to the melting point of the system. This result supports the T_m predicted from the thermal properties. At 770 K above the melting point, the PDF shows the characteristic behavior of the completely liquid phase.

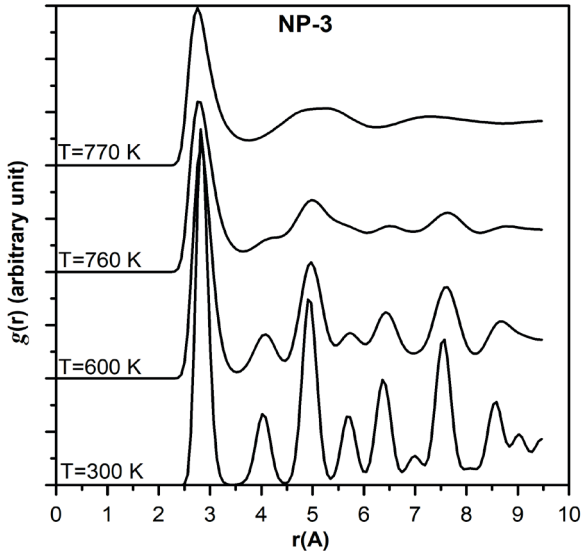

Fig. 3. *PDFs of Al NP-3 at different temperatures during the heating process.*

Information about the dynamic behavior of the NP during the melting process can be obtained by analyzing physical properties such as the diffusion coefficient and MSD. The diffusion coefficients of the atoms forming the NP, D, are calculated by using the Einstein equation [17]:

$$D = \lim_{t\to\infty} \frac{MSD}{6t} \quad (3)$$

where t is the diffusion time, MSD of the atom in the MD simulations can be described as [17]:

$$MSD = \frac{1}{N}\sum_{i=1}^{N} \left| r_i(t + t_o) - r_i(t_o) \right|^2 \quad (4)$$

where $r_i(t_o)$ is the position vector of the ith atom for the system in its initial configuration and $r_i(t)$ is the position vector of ith atom at time t. The change of MSDs calculated for Al NP-3 at different temperatures with respect to time is plotted

in Figure 4. At 300 K and 600 K, the MSD curves exhibit crystal-like characteristic behavior. There is a significant increase in the slope of the MSD curve at T_m=760 K. This increase is a dynamic indicator that there are both liquid-like structures and solid-like structures in the system at the melting point. This result supports the melting behavior observed in the static structure. The slope of the MSD curve increased even more at 770 K above the melting point. This indicates that all atoms constituting the NP exhibit liquid-like dynamic properties.

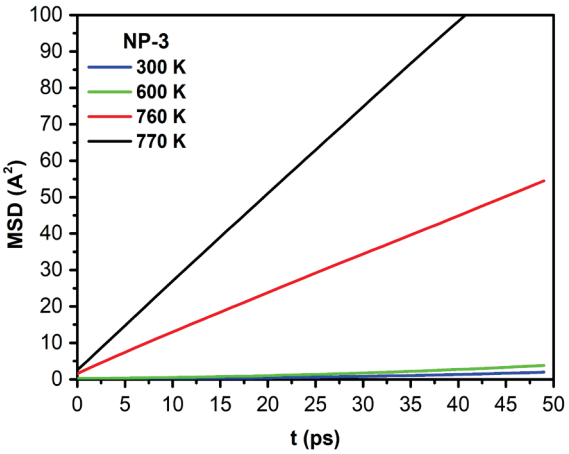

Fig. 4. *Time-dependent changes of MSDs obtained at different temperatures for Al NP-3.*

The diffusion coefficients calculated from the MD simulations for Al NPs and bulk system are plotted as a function of temperature in Figure 5. The diffusion coefficients of all NPs and bulk system increase abnormally at their melting points. This increase shows that the atoms forming the system are mobilized in the system by getting rid of their lattice points. In other words, each system starts to melt at the melting point and exhibits liquid-like behavior. Thus, the accuracy of the melting points estimated from thermal properties was tested once again with the characteristic behavior of dynamic properties. After the melting point, the diffusion coefficients of NP-1 and NP-2, which are smaller in size, are larger than those of NP-3 and show large oscillations with increasing temperature. However, for NP-3, diffusion coefficient increases linearly with temperature after the melting point and shows similar behavior to the bulk system. This situation can be explained by the fact that the atoms forming the NP are more thermally unstable since the surface area to volume ratio increases as the particle size decreases.

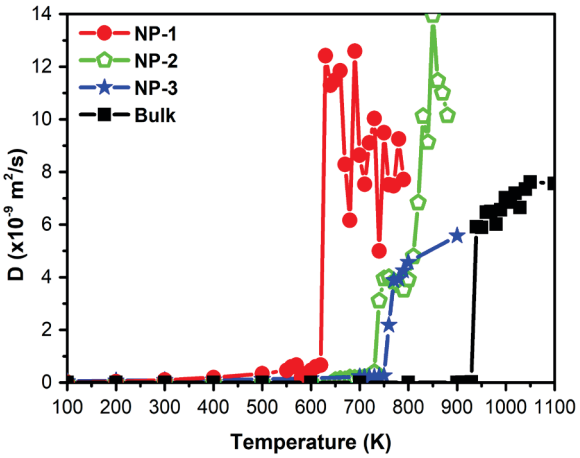

Fig. 5. *Temperature-dependence of diffusion coefficient for Al NPs and bulk system.*

The snapshots of the atomic configuration during the melting process can provide important information about the dynamic process of the NP. In this context, the snapshot atomic images obtained from the MD simulation at different temperatures Al NP-3 are given in Figure 6.

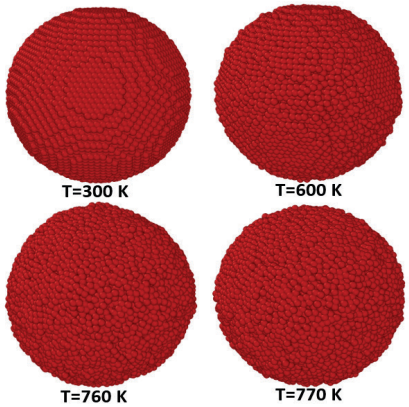

Fig. 6. *Snapshots of NP-3 at different temperatures during the melting process.*

As can be seen from the snapshots, the atomic arrangement on the NP surface at 300 K is in an ideal fcc crystal structure. At 600 K, the surface atoms begin to leave the lattice points due to the temperature

increase due to the lack of bonds and the existing metallic bonds begin to break. This is an indication that pre-melting has begun in the surface region of the NP before the melting point. At the melting point, at 760 K, the atomic order in the surface region of the NP is completely disrupted and a liquid-like layer is formed. At 770 K, the NP melts homogeneously and the atoms have liquid-like atomic motion.

CONCLUSION

In this work, the structural and dynamic properties of Al NPs during the melting process were investigated using classical MD simulation with EAM potentials. Results from MD simulations showed that particle size not only changes the thermal properties of the NP but also dramatically changes its structural and dynamic properties. The melting point and heat of fusion of the NP increase with increasing particle size and are lower than those of the bulk for all NPs. Dynamic properties show that even in the low temperature region, the thermal stability of NP-1 and NP-2 is poorer than NP-3. At temperatures above the melting point, as the particle size decreases, significant oscillations in the diffusion coefficient occur, while these oscillations disappear as the size increases. Additionally, at temperatures lower than the melting point, a pre-melting occurs on the surface of the NP.

Funding: No funding support has been received from any institution or person.
Acknowledgments: We would like to thank Trakya University Rectorate for giving permission and contributing to present this study as a paper.

REFERENCE

[1] A. V. Fedorov, A. V. Shulgin, Mathematical modeling of melting of nano-sized metal particles, Combust. Explos. Shock Waves 47 (2011) 147–152.
[2] A. V. Fedorov, A. V. Shulgin, S.A. Lavruk, Description of melting of aluminum nanoparticles, Combust. Explos. Shock Waves 52 (2016) 457–462.
[3] J. Liu, M. Wang, P. Liu, Molecular dynamical simulations of melting Al nanoparticles using a reaxff reactive force field, Mater. Res. Express 5 (2018) 065011.
[4] I.A. Bedarev, S.A. Lavruk, Study of the Dependence of the Melting Temperature of Aluminum Nanoparticles on the Particle Size, J. Eng. Phys. Thermophys. 95 (2022) 1672–1676.
[5] Y.-S. Kwon, A.A. Gromov, A.P. Ilyin, E.M. Popenko, G.-H. Rim, The mechanism of combustion of superfine aluminum powders, Combust. Flame 133 (2003) 385–391.
[6] P. Puri, V. Yang, Effect of Particle Size on Melting of Aluminum at Nano Scales, J. Phys. Chem. C 111 (2007) 11776–11783.
[7] J. Novak, Molecular dynamics simulation of aluminium melting, Mater. Geoenvironment 63 (2016) 9–18.
[8] M.S. Daw, M.I. Baskes, Embedded-atom method: Derivation and application to impurities, surfaces, and other defects in metals, Phys. Rev. B 29 (1984) 6443–6453.
[9] H. Sheng, EAM potentials, (2024). https://sites.google.com/site/eampotentials/table/al.
[10] W. Smith, T.R. Forester, DL_POLY_2.0: A general-purpose parallel molecular dynamics simulation package, J. Mol. Graph. 14 (1996) 136–141.
[11] C. Kittel, Introduction to the physics of the solid state, University, John Wiley & Sons, Inc, 1986.
[12] S. Nose, A unified formulation of the constant temperature molecular dynamics methods, J. Chem. Phys. 81 (1984) 511.
[13] H.J.C. Berendsen, J.P.M. Postma, W.F. van Gunsteren, A. DiNola, J.R. Haak, Molecular dynamics with coupling to an external bath, J. Chem. Phys. 81 (1984) 3684–3690.
[14] Metals-heat of fusion, (2024). https://www.engineeringtoolbox.com/fusion-heat-metals-d_1266.html.
[15] U. Domekeli, A molecular dynamic study of the effects of high pressure on the structure formation of liquid metallic $Ti_{62}Cu_{38}$ alloy during rapid solidification, Comput. Mater. Sci. 187 (2021) 110089.
[16] Y. Waseda, "The Structure of Non-Crystalline Materials, Liquid and Amorphous Solid, McGraw-Hill, New York., 1980.
[17] S. Dalgic, U. Domekeli, Melting properties of tin nanoparticles by molecular dynamics simulation, J. Optoelectron. Adv. Mater. 11 (2009) 2126–2132.